CONSISTENT SMALL-SIGNAL AND RF-NOISE PARAMETER MODELLING OF CARBON DOPED INP/INGAAS HBT

Michael Agethen, Silja Schüller, Peter Velling, Wolfgang Brockerhoff, Franz-Josef Tegude

Gerhard-Mercator-University Duisburg, Solid-State Electronics Dept., 47057 Duisburg, Germany

Abstract - **In this work a consistent small-signal and rf-noise parameter model of InP/InGaAs HBT is presented. This model is based on the typical three-mesa design of HBT and correlates intrinsic noise sources to specific device regions. Bias dependent investigation of s- and rf-noise parameters proves the consistency of the model.**

I. INTRODUCTION

The design of complex high-frequency analog electronic circuits is very difficult and strongly depends on the models used for the single device. These models have to take into account all relevant physical phenomena, which may influence the circuit performance, and was done for InP based HFET years before [1]. In case of HBT quantitative small-signal modelling has been done, but the modelling of rf-noise parameters (minimum noise figure F_{min}, noise equivalent resistance R_n and optimum generator reflection coefficient $\underline{\Gamma}_{opt}$) is critical, because e.g. not all noise parameters can be described by established models [2]. Usually models are based on two correlated noise current sources for collector current I_C and base current I_B and the correlation coefficient of both sources has to be determined [3]. Unfortunately no information of intrinsic noise sources of the device is included. As a result the consistency of small-signal and noise equivalent circuit is difficult to achieve. The method presented in this paper uses a physically relevant "T"-like small-signal equivalent circuit instead of "π"-like model for small-signal as well as noise modelling, which correlates various intrinsic noise sources to specific HBT device regions.

II. THE CONSISTENT SMALL-SIGNAL AND RF-NOISE PARAMETER EQUIVALENT CIRCUIT

Fig. 1 shows the extended small-signal equivalent circuit of HBT, which builds up the basis of the new consistent small-signal and rf-noise parameter model. This "T"-like equivalent circuit can easily be found considering the typical three-mesa design of III-V semiconductor based HBT [4]. In case of narrow band noise, equivalent noise temperatures are associated with all resistances. In fig. 1 all equivalent noise temperatures are included. As usual the small-signal model is divided into two parts, an intrinsic and an extrinsic one. The extrinsic resistances only add thermal noise, consequently their equivalent noise temperature is set to the ambient temperature T_A. The noise from the included RC-combination R_{BP} and C_{BP} at the base contact (fig. 1), taking into account a frequency dependence of the non alloyed ohmic base contact, is assumed to be thermal noise, too. As a consequence only the four intrinsic equivalent noise temperatures have to be found for a complete rf-noise parameter modelling of HBT. Additionally, with the help of these noise temperatures, a localisation of various noise sources and phenomena in specific HBT regions is possible.

To model the rf-noise parameters of the HBT, the noise correlation matrix of the complete circuit has to be calculated. This can be done by replacing all noisy resistances with their one-port noise equivalent circuit, a noise current source in parallel or a noise voltage source in

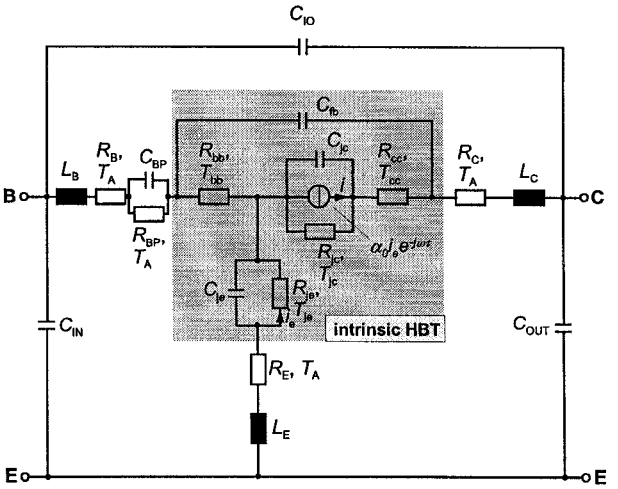

Fig. 1. Consistent small-signal and rf-noise parameter equivalent circuit of InP/InGaAs HBT.

series to the noise free resistance. Fig. 2 shows the intrinsic HBT model in more detail. In case of the very inner part of the model, the noisy resistances of the base-emitter junction R_{je} and the base collector junction R_{jc} are replaced by their noise current sources. The resistances itself are now noise free.

The noise correlation matrix in admittance form of this inner HBT part

$$\ddot{C}_Y = \begin{pmatrix} C_{Y_{11}} & C_{Y_{12}} \\ C_{Y_{21}} & C_{Y_{22}} \end{pmatrix} \quad (1)$$

can be calculated as follows:

$$C_{Y_{11}} = \left|i_{jc}\right|^2 + (1+\alpha_0 \cdot (\alpha_0 - 2\cos(\omega\tau)) \cdot \left|i_{je}\right|^2 \quad (2)$$

$$C_{Y_{12}} = -\left|i_{jc}\right|^2 + \alpha_0 \cdot (\cos(\omega\tau) - \alpha_0 + j\sin(\omega\tau)) \cdot \left|i_{je}\right|^2 \quad (3)$$

$$C_{Y_{21}} = C_{Y_{12}}^{*} \quad (4)$$

$$C_{Y_{22}} = \left|i_{jc}\right|^2 + \alpha_0^{\,2} \cdot \left|i_{je}\right|^2 \quad (5)$$

with the spectral densities of both intrinsic noise current sources:

$$\left|i_{jc}\right|^2 = 4k\Delta f \frac{T_{jc}}{R_{jc}} \quad (6)$$

$$\left|i_{je}\right|^2 = 4k\Delta f \frac{T_{je}}{R_{je}} \quad (7)$$

In case of narrow band noise the bandwidth used for calculation is equal to $\Delta f = 1$ Hz.

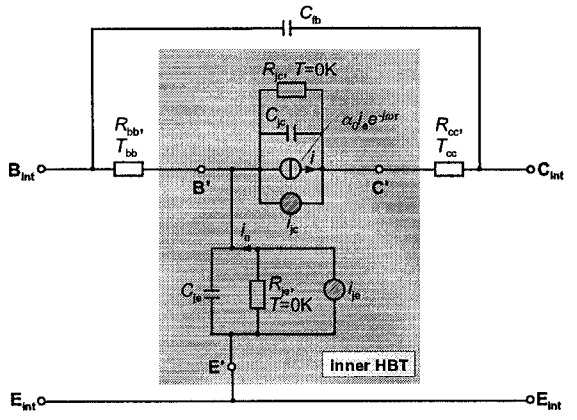

Fig. 2. Intrinsic part of the consistent small-signal and rf-noise parameter model. The noisy elements of the inner part are replaced by their one-port noise equivalent circuit.

After calculating this inner noise correlation matrix all other parts of the model can be embedded using well known transformation rules for noise correlation matrices [5] and noise circuit theory of two-ports [3].

For modelling the HBT rf-parameters, all equivalent circuit elements (small-signal elements and equivalent noise temperatures) are optimised using evolutionary optimisation strategies. These strategies combine deterministic and stochastic search algorithm, so these approaches are independent of the initial optimisation values. Evolutionary optimisation has demonstrated its performance in high dimensional optimisation problems and results in the global optimum [6].

III. Measurement Set-up and Investigated Devices

Using an on-wafer measurement set-up in combination with commercial HP8510C s-parameter and ATN NP5 rf-noise parameter analyser, both s-parameter and rf-noise characterisation is performed in a frequency range from 45 MHz up to 40 GHz and 1 GHz up to 18 GHz, resp.. Devices under test are carbon doped InP/InGaAs non self-aligned HBT with an emitter area $A_E = 30\mu m^2$, grown by LP-MOVPE with non gaseous sources (TBAs/TBP, DitBuSi/CBr4, TMIn/TEGa) in nitrogen carrier gas. The carbon doped p-(InGa)As:C base ($p > 10^{19} cm^{-3}$) is compositionally graded to increase current gain (here: $B > 300$) and transit frequency (here: $f_T > 65$ GHz and $f_{max} > 35$ GHz) and a high temperature in-situ annealing sequence is carried out in TMAs/N2 ambient at $T > 600°C$ to activate the carbon doping in the base [7].

IV. RF-Parameter Modelling

As a first result fig. 3 shows the excellent capability of the model used to describe s-parameters of HBT in the whole measured frequency range up to 40 GHz. Here, the measured and modelled s-parameters at collector-emitter voltage $V_{CE} = 1.2$ V in active device region and collector current $I_C = 10$ mA are presented. The symbols represent the measured data, the solid lines the modelled values. Bias dependent measurements are performed and the good agreement between measured and modelled data was achieved.

To prove the consistency with rf-noise parameter modelling, fig. 4 to fig. 6 show the measured and modelled rf-noise parameters for three different bias conditions at constant collector-emitter voltage $V_{CE} = 1.2$ V and various collector currents from $I_C = 1$ mA up to $I_C = 20$ mA. The small-signal equivalent elements are extracted by small-signal modelling and kept constant

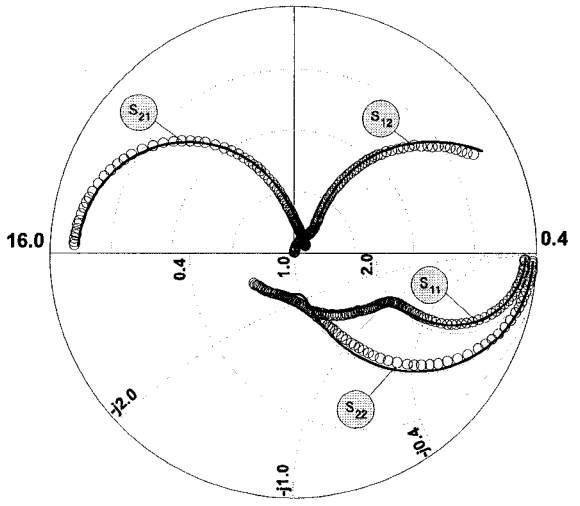

Fig. 3. Measured (symbols) and modelled (lines) s-parameters in frequency range from 45 MHz up to 40 GHz at $V_{CE} = 1.2$ V and $I_C = 10$ mA (s_{11} and s_{22} in Smith-Chart, s_{12} and s_{21} in polar diagram).

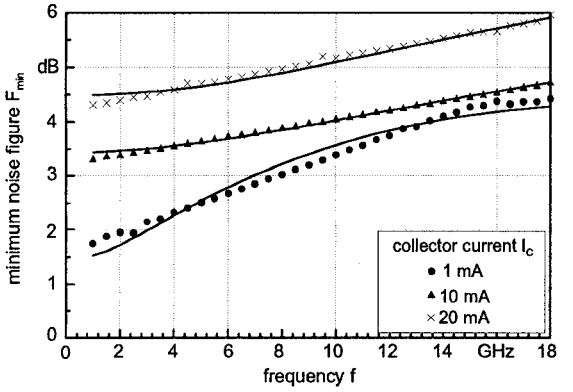

Fig. 4. Measured (symbols) and modelled (lines) minimum noise figure in frequency range from 1 GHz up to 18 GHz at constant $V_{CE} = 1.2$ V.

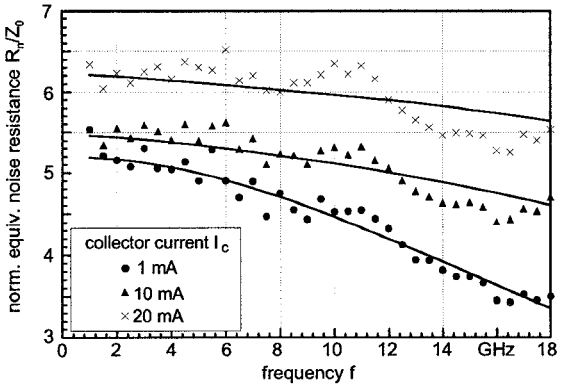

Fig. 5. Measured (symbols) and modelled (lines) normalized equivalent noise resistance $r_n = R_n/Z_0$ in frequency range from 1 GHz up to 18 GHz at constant $V_{CE} = 1.2$ V.

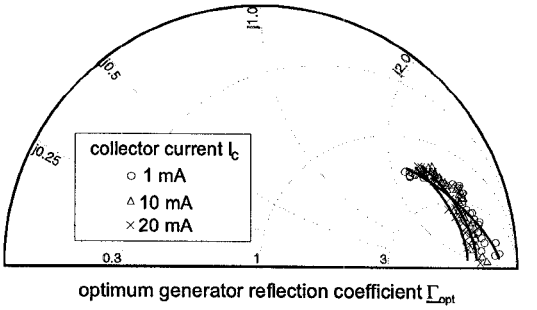

Fig. 6. Measured (symbols) and modelled (lines) optimum generator refection coefficient $\underline{\Gamma}_{opt}$ in frequency range from 1 GHz up to 18 GHz at constant $V_{CE} = 1.2$ V.

during noise-parameter optimisation. Only the four intrinsic noise equivalent temperatures are optimised.

First of all the excellent agreement between measured and modelled data can clearly be seen for all three noise parameters. For the minimum noise figure F_{min}, a strong increase with rising collector current is obvious (fig. 4). The normalized equivalent noise resistance $r_n = R_n/Z_0$ (fig. 5) shows the same dependence on collector current I_C. A minor influence of the collector current is found for the optimum generator reflection coefficient $\underline{\Gamma}_{opt}$ (fig. 6).

V. Investigation of Intrinsic Noise Sources

As a result of the above mentioned small-signal and rf-noise parameter model a localization of various noise sources in the specific device regions is possible. With the optimisation results, the spectral densities of the four intrinsic noise current sources can be calculated and investigated in dependence of bias condition. The following formula is used for calculation of the intrinsic noise currents due to optimised model parameter values, here resistance R_x and equivalent noise temperature T_x (with index "x" for all various intrinsic noise sources):

$$i_{x,n} = \sqrt{4k\frac{T_x}{R_x}} \tag{8}$$

These calculated values are now plotted in dependence on bias condition, here we calculate the base $i_{B,S}$ and collector $i_{C,S}$ shot noise currents due to dc values with:

$$i_{B,S} = \sqrt{2eI_B} \tag{9}$$

$$i_{C,S} = \sqrt{2eI_C} \tag{10}$$

Fig. 7 shows the intrinsic base noise current $i_{bb,n}$ in dependence on base shot noise current $i_{B,S}$. The intrinsic

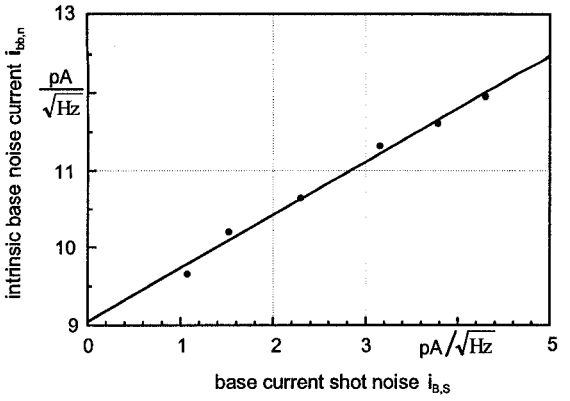

Fig. 7. Extracted (•) intrinsic base noise currents in dependence on base current shot noise at constant V_{CE} = 1.2 V. Solid line represents linear fit.

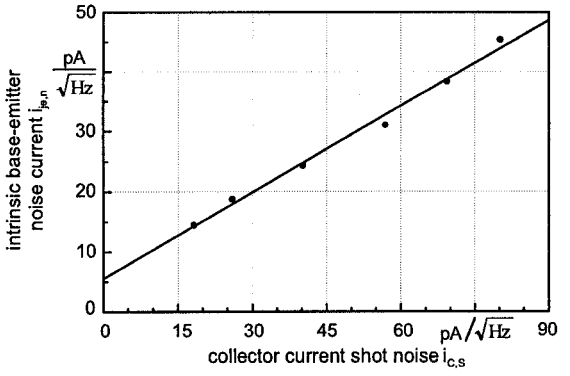

Fig. 8. Extracted (•) intrinsic base-emitter junction noise currents in dependence on collector current shot noise at constant V_{CE} = 1.2 V. Solid line represents linear fit.

base noise current shows a linear dependence on extrinsic dc base current. But a very high offset is obvious, which is correlated to the intrinsic base noise source and has to be investigated in more detail.

Fig. 8 now shows the intrinsic base-emitter junction noise current $i_{je,n}$ in dependence on collector shot noise $i_{S,C}$. This intrinsic noise source depends linearly on collector current I_C.

The two last intrinsic noise current sources show only minor influence and bias dependence. The intrinsic base-collector noise current $i_{jc,n}$ is equal to the shot noise current of the dc base current (comp. fig. 9). The values of intrinsic collector noise current $i_{cc,n}$ are very low and independent on extrinsic currents. As a consequence the intrinsic noise source due to collector resistance can be neglected.

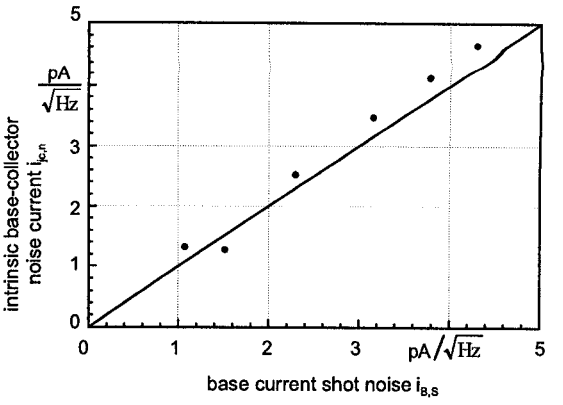

Fig. 9. Extracted (•) intrinsic base-collector junction noise currents in dependence on base current shot noise at constant V_{CE} = 1.2 V. Solid line represents linear fit.

VI. Conclusion

A consistent small-signal and rf-noise parameter model of InP/InGaAs HBT is presented. The excellent agreement between measured and modelled rf-parameters is clearly demonstrated and a localization of intrinsic noise sources to specific device regions is made and investigated in more detail.

References

[1] R. Reuter et al., "Investigation and modeling of impact ionization with regard to the RF- and noise behaviour of HFET", IEEE Trans. Microwave Theory Tech., vol. 45, pp. 977-983, 1997

[2] A. Huber et al., "RF Noise Characterization of a high performance InP/InGaAs HBT", Conf. Proc. of the 20th Workshop Compound Semiconductor Device Integr. Circuits, 1996, Lithuania, pp. 83-84

[3] H. Rothe, W. Dahlke, "Theory of noisy fourpoles", Proceedings of the IRE, vol. 44, pp. 811-818, 1956

[4] D. Peters et al., "RF-Characterization of AlGaAs/GaAs HBT down to 20 K", Proc. of the 20th Int. Symp. on GaAs and Related Compounds, Freiburg, Germany, Aug. 1993, pp. 177-182

[5] H. Hillbrand, P. H. Russer, "An efficient method for computer aided noise analysis of linear networks", IEEE Transactions on Circuits and Systems, CAS-23, pp. 235-238, 1976

[6] M. Agethen et al., "Small-Signal Modelling of HBT Using Evolutionary Multi-Bias Optimization Algorithm", Proc. Of 11th III-V Semiconductor Device Simulation Workshop, IEMN, Villeneuve d'Ascq, France, May 1999

[7] P. Velling, "A comparative study of GaAs- and InP-based HBT growth by means of LP-MOVPE using conventional and non gaseous sources", to be published in "Progress in Crystal Growth and Characterization of Materials", Dec. 2000.